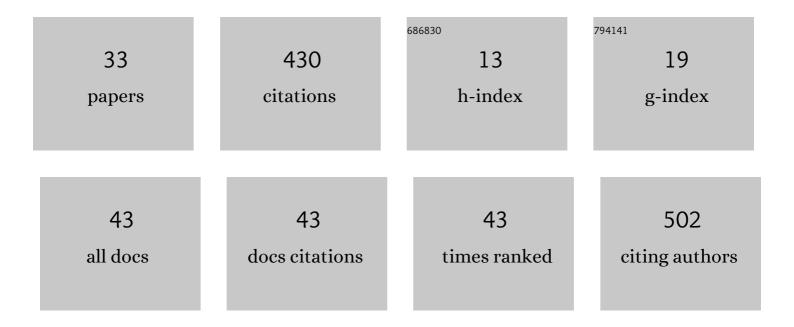
Gabriel B Hall

List of Publications by Year in descending order

Source: https://exaly.com/author-pdf/4403664/publications.pdf Version: 2024-02-01



CARDIEL R HALL

#	Article	IF	CITATIONS
1	Intramolecular Electron Transfer in Bipyridinium Disulfides. Journal of the American Chemical Society, 2014, 136, 4012-4018.	6.6	40
2	Closing the Nuclear Fuel Cycle with a Simplified Minor Actinide Lanthanide Separation Process (ALSEP) and Additive Manufacturing. Scientific Reports, 2019, 9, 12842.	1.6	37
3	Nitric Acid and Water Extraction by T2EHDGA in <i>n</i> -Dodecane. Solvent Extraction and Ion Exchange, 2017, 35, 586-603.	0.8	31
4	An Advanced TALSPEAK Concept for Separating Minor Actinides. Part 1. Process Optimization and Flowsheet Development. Solvent Extraction and Ion Exchange, 2017, 35, 377-395.	0.8	26
5	Rational Design of Rhodium Complexes Featuring ΰ ⁴ â€ <i>N</i> , <i>N</i> , <i>N</i> , <i>N</i> , <i>N</i> , ―and ΰ ⁵ â€ <i>N</i> , <i>N</i> , <i>N</i> , <i>P</i> , <i>P</i> , <i>P</i> , <i>Bis(imino)pyridine Ligands. European Journal of Inorganic Chemistry, 2013, 2013, 4430-4442.</i>	1.0	23
6	Simulant testing of a co-decontamination (CoDCon) flowsheet for a product with a controlled uranium-to-plutonium ratio. Separation Science and Technology, 2019, 54, 1977-1984.	1.3	23
7	Sensor Fusion: Comprehensive Real-Time, On-Line Monitoring for Process Control via Visible, Near-Infrared, and Raman Spectroscopy. ACS Sensors, 2020, 5, 2467-2475.	4.0	23
8	Electrochemical, Spectroscopic, and Computational Study of Bis(μ-methylthiolato)diironhexacarbonyl: Homoassociative Stabilization of the Dianion and a Chemically Reversible Reduction/Reoxidation Cycle. Organometallics, 2014, 33, 5009-5019.	1.1	21
9	Extraction Behavior of Ln(III) Ions by T2EHDGA/ <i>n</i> -Dodecane from Nitric Acid and Sodium Nitrate Solutions. Solvent Extraction and Ion Exchange, 2018, 36, 331-346.	0.8	21
10	Redox Chemistry of Noninnocent Quinones Annulated to 2Fe2S Cores. Organometallics, 2013, 32, 6605-6612.	1.1	19
11	Evolution of Acid-Dependent Am ³⁺ and Eu ³⁺ Organic Coordination Environment: Effects on the Extraction Efficiency. Inorganic Chemistry, 2020, 59, 4453-4467.	1.9	19
12	Surprising formation of quasi-stable Tc(<scp>vi</scp>) in high ionic strength alkaline media. Inorganic Chemistry Frontiers, 2018, 5, 2081-2091.	3.0	15
13	Identification and Quantification of Technetium Species in Hanford Waste Tank AN-102. Analytical Chemistry, 2020, 92, 13961-13970.	3.2	14
14	Overcoming Oxidation State-Dependent Spectral Interferences: Online Monitoring of U(VI) Reduction to U(IV) via Raman and UV–vis Spectroscopy. Industrial & Engineering Chemistry Research, 2020, 59, 8894-8901.	1.8	13
15	Theoretical Modeling of ⁹⁹ Tc NMR Chemical Shifts. Inorganic Chemistry, 2016, 55, 8341-8347.	1.9	10
16	Spectroscopic Characterization of Aqua [<i>fac</i> -Tc(CO) ₃] ⁺ Complexes at High Ionic Strength. Inorganic Chemistry, 2018, 57, 6903-6912.	1.9	10
17	Characterization of spent Purolite A530E resin with implications for long-term radioactive contaminant removal. Journal of Environmental Chemical Engineering, 2020, 8, 104155.	3.3	8
18	Spontaneous redox continuum reveals sequestered technetium clusters and retarded mineral transformation of iron. Communications Chemistry, 2020, 3, .	2.0	8

GABRIEL B HALL

#	Article	IF	CITATIONS
19	Equatorial Electronic Structure in the Uranyl Ion: Cs ₂ UO ₂ Cl ₄ and Cs ₂ UO ₂ Br ₄ . Inorganic Chemistry, 2022, 61, 3821-3831.	1.9	8
20	Synthesis and characterization of [FeFe]-hydrogenase mimics appended with a 2-phenylazopyridine ligand. Journal of Sulfur Chemistry, 2013, 34, 566-579.	1.0	7
21	Improved Synthesis of 10-(2-Alkylamino-2-oxoethyl)-1,4,7,10-tetraazacyclododecane-1,4,7-triacetic Acid Derivatives Bearing Acid-Sensitive Linkers. Synthetic Communications, 2014, 44, 441-449.	1.1	6
22	Redox-Based Electrochemical Affinity Sensor for Detection of Aqueous Pertechnetate Anion. ACS Sensors, 2020, 5, 674-685.	4.0	6
23	Through space interaction between ferrocenes mediated by a thioether. Polyhedron, 2015, 86, 125-132.	1.0	5
24	Inorganic Ba–Sn nanocomposite materials for sulfate sequestration from complex aqueous solutions. Environmental Science: Nano, 2018, 5, 890-903.	2.2	5
25	Neighboring π-Amide Participation in Thioether Oxidation: Conformational Control. Organic Letters, 2016, 18, 3522-3525.	2.4	4
26	Unveiling the Early Stages of the F-element Oxalate Growth Evolution with Cryo-TEM. Microscopy and Microanalysis, 2020, 26, 642-644.	0.2	3
27	Molar absorptivities of U(VI), U(IV), and Pu(III) in nitric acid solutions of various concentrations relevant to developing nuclear fuel recycling flowsheets. Journal of Radioanalytical and Nuclear Chemistry, 2020, 324, 773-789.	0.7	3
28	Optical Spectroscopic Investigation of Hexavalent Actinide Ions in n-Dodecane Solutions of Tri-butyl Phosphate. Solvent Extraction and Ion Exchange, 2021, 39, 56-73.	0.8	2
29	tert-Butyl 4-(3,4-dichloroanilino)piperidine-1-carboxylate. Acta Crystallographica Section E: Structure Reports Online, 2013, 69, o205-o205.	0.2	1
30	Two organophosphorus pesticides: methyl parathion and dicapthon. Acta Crystallographica Section C, Structural Chemistry, 2014, 70, 975-977.	0.2	0
31	Correlative Microscopic, Spectroscopic, and Computational Analysis of the Nucleation and Growth of Europium (III) Oxalate Nanoparticles. Microscopy and Microanalysis, 2016, 22, 1396-1397.	0.2	0
32	Cryo-TEM Characterization of the Early Stages of the Uranium Oxalate Growth Evolution. Microscopy and Microanalysis, 2021, 27, 1940-1941.	0.2	0
33	3-(4-Bromophenyl)-1-butyl-5-[1-(2-chloro-6-methylphenyl)-1H-tetrazol-5-yl]imidazolidine-2,4-dione. Acta Crystallographica Section E: Structure Reports Online, 2013, 69, o1102-o1103.	0.2	0